Pure Green synthesis and characterization of carbon dot cluster nanofluid from mango leaves

Kalaiarasi G[1], Sundarrajan Marimuthu[2], Anbuselvan C S[3]
[1,2,3]*Department of Physics, Sri Chandrasekharendra Saraswathi Viswa Mahavidyalaya, Enathur, Kanchipuram, India.*
http://doi.org/10.64643/IJIRTV12I5-185852-459

***Abstract*—This study presents a green thermal pyrolysis method for synthesizing carbon nanofluids from mango leaves (Mangifera indica) biomass under low oxygen conditions. Fresh mango leaves were processed to obtain a powder, which was subjected to controlled pyrolysis at 250 °C to yield carbonaceous material. The resulting charcoal was dispersed and filtered in aqueous media to produce carbon dot cluster (CDC) nanofluids. Comprehensive characterization using FTIR revealed abundant hydroxyl, amide, carboxyl, and aromatic functionalities, while UV-Vis absorption displayed four peaks (199, 210, 241, 300 nm), confirming conjugated carbon cores and surface functionalization essential for photonic applications. XRD analysis identified broad amorphous peaks with graphitic domains, as well as minor crystalline and metal oxide phases, indicating a hybrid nanostructure. DLS results showed a major particle fraction at 85.78 nm with additional aggregates, and zeta potential measurements indicated moderate colloidal stability (–18.1 mV). These findings demonstrate that mango leaf-derived carbon CDC nanofluids possess diverse optical and chemical properties, making them promising candidates for sustainable thermal management and catalytic applications.**

***Index Terms*—Biomass-derived nanomaterials, Carbon dot clusters, Colloidal stability, Dynamic light scattering, FTIR spectroscopy, Green synthesis, Mango leaf nanofluid, Pyrolysis, UV–Vis absorption, X-ray diffraction, Zeta potential.**

I. INTRODUCTION

Nanoparticles, typically described as materials with at least one dimension ranging from 1 to 100 nanometers, manifest unique physicochemical and biological characteristics compared to their bulk counterparts, mainly due to their elevated surface-to-volume ratio and quantum confinement behavior [1, 2]. These nanoscale traits have accelerated their adoption in numerous disciplines such as catalysis, biomedicine, energy devices, and environmental engineering [3]. Broadly, nanoparticle fabrication is achieved through two main strategies—top-down and bottom-up. In the top-down route, physical forces such as mechanical milling or laser ablation reduce bulk materials into finer particles [4, 5]. By contrast, the bottom-up technique relies on controlled atomic or molecular assembly using chemical processes like sol-gel and hydrothermal synthesis [6]. The chosen fabrication method profoundly influences particle morphology, distribution, and reproducibility in large-scale production.

Nanomaterials are further classified as metallic, polymeric, or composite systems. Metallic nanoparticles—including materials like gold, silver, and copper—are noted for high electrical conductivity, catalytic reactivity, and antimicrobial potential, thereby finding use in electronics and biomedical applications [7,8]. Polymeric nanomaterials, known for flexibility and biocompatibility, serve effectively in coatings and drug delivery systems [9]. Composite nanomaterials, which merge multiple phases, exhibit improved mechanical integrity and thermal resistance suitable for aerospace and structural applications [10] . Recently, carbon-integrated hybrids have drawn attention for combining the electrical versatility of carbon with enhanced catalytic and structural features inherited from dopants or polymeric matrices [11,12]

The remarkable behavior of nanomaterials arises from their structured surfaces, broad functional group diversity, and tunable electronic band characteristics. Carbon-derived nanostructures—such as carbon dots or graphene-based materials—demonstrate high luminescence efficiency, establishing their importance in sensing and bioimaging [13.14]. Similarly, metal-based nanoparticles are leveraged for photocatalytic and antimicrobial activity, beneficial in water purification and therapeutic formulations [15]. Nanofluids, defined as colloidal dispersions of nanoparticles within a fluidic medium, have emerged as a promising technological category. The inclusion of nanoparticles such as oxides,

carbons, or metals in solvents like water, ethylene glycol, or oils drastically enhances thermal conductivity, viscosity regulation, and overall heat transfer performance [16,17]. Nanofluids are commonly fabricated using one-step and two-step methodologies. The one-step approach directly forms nanoparticles in situ within the desired fluid, offering stable dispersions, while the two-step approach—where pre-synthesized nanoparticles are dispersed—remains more scalable and economically feasible [18,19] . Stabilization of such dispersions often involves surfactant incorporation, ultrasonication, or surface modification treatments to mitigate agglomeration tendencies [20].

Among nanofluids, carbon-based systems such as those comprising carbon dots, graphene oxide, or carbon nanotubes are gaining traction due to their optical tunability, high stability, and biocompatibility [21,22] . These fluids exhibit superior dispersibility, reduced cytotoxicity, and notable photothermal conversion efficiency, supporting their role in renewable energy harnessing, biomedical imaging, and thermal regulation [23,24]. Compared to traditional metal oxide nanofluids (e.g., Al2O3, TiO2), carbon nanofluids generally exhibit reduced sedimentation and improved colloidal stability because of their lower density and higher surface activity [25] .

Green synthesis offers a sustainable alternative to conventional chemical or physical methods by employing natural biomolecules as reducing and stabilizing agents, thereby limiting toxic reagents and minimizing energy usage [26,27] . Plant-derived precursors, including fruit peels, leaves, seeds, and algal biomass, have proven valuable for producing stable, functional carbon nanostructures [28-30] . Examples include reports on banana peels, neem leaves, and aloe vera extracts being successfully utilized for synthesizing luminescent carbon dots and thermally enhanced nanofluids [31,32].

Recently, the demand for biomass-based nanofluids has risen, aligning with resource circularity and green manufacturing initiatives. Agricultural wastes—such as leaves, husks, and shells—are recognized as renewable, low-cost carbon precursors, enabling both environmental and economic advantages [33]. Such green approaches provide dual benefits—reducing waste while generating materials for advanced energy, catalytic, and biomedical technologies [34].

In this context, nanofluids demonstrate high potential in energy transfer, thermal regulation, and biomedical processes because of their superior stability and conductivity profiles . Carbon nanofluids derived from lightweight nanostructures like carbon dots and nanotubes further extend applications in photothermal systems, catalytic reactions, and imaging platforms [35-38] .

The present study focuses on developing a purely green, thermal pyrolysis-based synthesis of carbon dot clusters (CDC) utilizing mango leaves (Mangifera indica) as a biomass source under limited oxygen conditions. The objective is to formulate stable, aqueous CDC nanofluids for potential implementation in photothermal and energy management applications.

II. MATERIALS AND METHODS

2.1 Materials

Fresh Mango leaves (Mangiferaindica) were collected locally from gardens in Kancheepuram, Tamil Nadu, India. No reagents were used and only double distilled water was used throughout all processes.

2.2 Preparation of mango leaf powder

The mango leaves were washed repeatedly with distilled water to remove surface impurities. The cleaned leaves were dried under sunlight, protected in a covered environment, and then finely ground using a mechanical grinder to yield uniform powder.

Fig.2.1. Mango leaf powder

2.3 Synthesis of charcoal by thermal pyrolysis

The powdered mango leaves were subjected to thermal pyrolysis in a controlled environment with minimal oxygen supply to permit carbonization without combustion. Temperature was steadily increased to 250 °C and held constant to convert the biomass into charcoal.

Fig.2.2. CDC nanopowder

2.4 Preparation of carbon dot cluster (CDC) Nanofluid

The obtained charcoal was dispersed in double distilled water under magnetic stirring. The suspension was initially filtered through Whatman filter no.1 to remove coarse particles, followed by filtration using a 0.22 μm syringe filter to ensure removal of aggregates and obtain a stable nanofluid. The final nanofluid was stored in airtight containers for further characterization and applications.

Fig.2.3. CDC nanofluid
[Under normal and UV light]

III. RESULTS AND DISCUSSION

3.1 FTIR Analysis

Results and discussion

The Fourier-transform infrared (FTIR) analysis provides comprehensive insight into the structural and surface functionalities of the synthesized carbon dot clusters. The prominent absorption at 3855 cm^{-1} may attributable to free hydroxyl (–OH) stretching vibrations, indicating the presence of unbound hydroxyl groups on the surface, which is consistent with literature reports highlighting hydroxyl-rich surface chemistries that enhance hydrophilicity and potential reactivity (39).

A broad and intense band centered at 3417 cm^{-1} corresponds to –OH/-NH stretching modes, which denote the hydroxyl/amide functionalities on the surface, a feature commonly observed in biogenic and green-synthesized carbon dots (40,41). These functional groups favor interactions with the environment and may contribute to the high stability and aqueous dispersibility of the nanomaterials.

Aliphatic C–H stretching vibrations at 2963 and 2930 cm^{-1} reaffirm the presence of methylene and methyl groups, indicative of residual organic moieties or surface passivating agents, aligning well with prior reports emphasizing these bands as markers of surface alkyl chains (42).

The absorption feature at 2216 cm⁻¹ arises from nitrile (C≡N) groups, suggesting either partial incorporation of nitrogen-containing precursors or surface-bound cyano functionalities. Although less frequently reported, such groups can modulate electronic properties and are noted in some advanced doped carbonaceous materials.

Strong absorptions at 1631 and 1574 cm⁻¹ are characteristic of carbonyl (C=O) and aromatic C=C stretching vibrations, respectively. The carbonyl groups reflect oxidized moieties or carboxylic acid functionalities, typical in carbon dot structures, while the aromaticC=C signals confirm graphitic or polyaromatic carbon domains within the materials (43). Secondary vibrational modes at 1410 and 1324 cm⁻¹, attributed to C–N stretching and C–H bending, further corroborate the presence of nitrogenous functionalities and alkyl groups, contributing to the multifunctional chemical dynamics of the nanosystems (44).

The moderate intensity band centered around 1111 cm⁻¹ corresponds to C–O stretching in alcohols, ethers, or esters, consistent with surface oxygenated species often introduced during hydrothermal or green synthesis methods (45).

Lower frequency absorptions, including 789 cm⁻¹ (aromatic C–H bending), 656 cm⁻¹ and 618 cm⁻¹

(skeletal or C–H bending modes), reinforce the complex chemical milieu comprising aromatic frameworks (46).

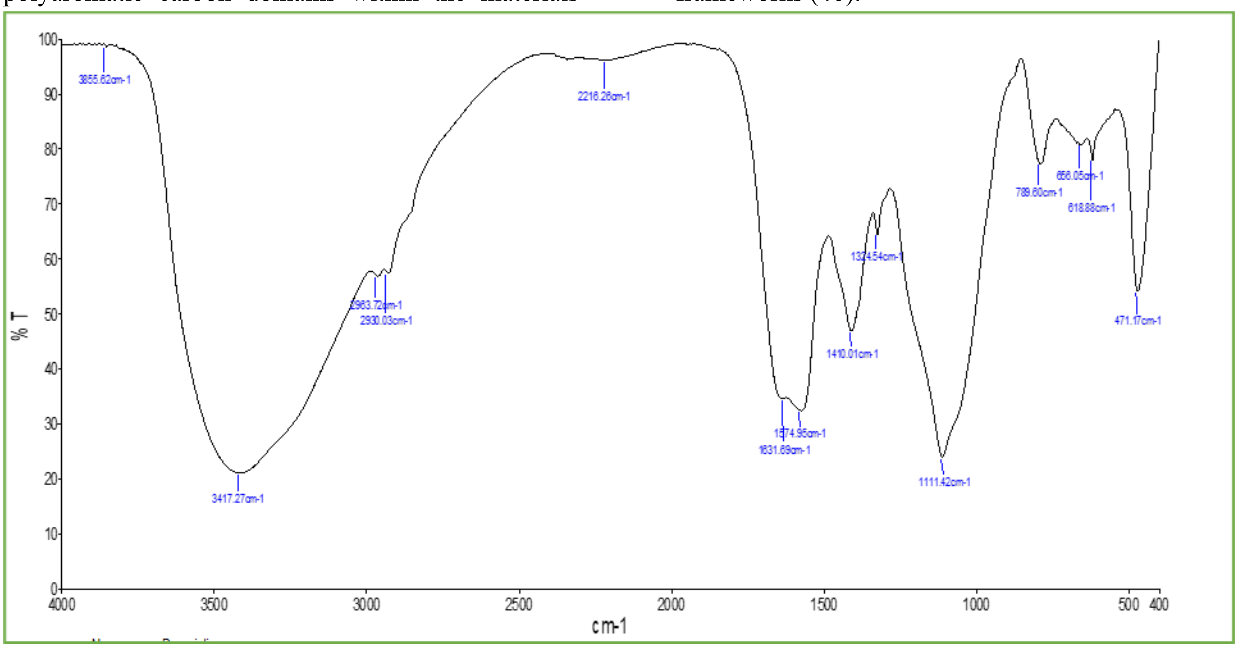

Fig.3.1. FTIR Spectrum of CDC nanofluid

Collectively, these FTIR signals paint a heterogeneous but well-defined surface landscape rich in oxygen- and nitrogen-containing functionalities, aromatic structures, and potential heteroatom dopants, aligning with the chemical signatures reported for green-synthesized carbon dots and their hybrids. Such structural attributes are pivotal for tuning the optical, electronic, and chemical properties of the nanomaterials, ultimately impacting their applications in sensing, catalysis, bioimaging, and environmental remediation as documented across the cited studies.

3.2 UV-Vis absorption analysis

Results and discussion

The UV-Vis spectrum shows four peaks with wavelengths at approximately 199 nm, 210 nm, 241 nm, and 300 nm. These peaks correspond to specific electronic transitions within the carbon nanodots in the clusters and help characterize their optical properties.

Fig.3.2 UV-Visible Spectrum of CDC nanofluid

The UV-Vis analysis of the carbon dot clusters reveals key absorption bands characteristic of conjugated carbon structures and surface functional groups. The absorption at 199 nm aligns with intense π–π* transitions in aromatic C=C bonds, consistent with the existence of extended conjugation within the carbon nanodot core, which enables efficient electron delocalization and robust optical responses (47).

The peak at 210 nm further confirms the aromatic character, representing π–π* electronic transitions in graphitic domains or extended π-conjugated systems, a hallmark of high-quality carbon dots synthesized via green methods. This absorption is essential for applications that rely on excitation of these conjugated systems, including fluorescence(47).

With increasing wavelength, the 241 nm peak corresponds to π–π* transitions involving poly aromatic / graphitic carbon units, with size-dependent quantum confinement effects influencing the absorption profile. This band is frequently reported in literature as a signature of mature carbon dot structure with well-formed graphitic networks (48).

Finally, the absorption near 300 nm arises from n–π* transitions associated with carbonyl and other oxygen- or nitrogen-containing surface functionalities. These surface groups modulate the nanodots' photophysical properties and contribute to their fluorescence behavior, reflecting successful surface functionalization and doping (47). Together, these absorption features demonstrate that the synthesized carbon dots possess well-defined aromatic cores with effective surface functionalization, matching reported green synthesis and functional nanocarbon literature. The consistent spectral features confirm the structural integrity and tunable optical characteristics critical for sensing, bioimaging, and photocatalytic applications.

3.3 XRD Analysis

Results and Discussion

The X-ray diffraction (XRD) pattern reveals a prominent broad peak at approximately 22.24° 2θ with an interplanar spacing of roughly 3.997 Å. This aligns well with the characteristic (002) reflection of amorphous carbonaceous materials featuring disordered graphite layers, consistent with the structure of green-synthesized carbon dots demonstrated in several studies. The breadth and slight asymmetry of this peak imply the presence of nanoscale graphitic domains interrupted by lattice

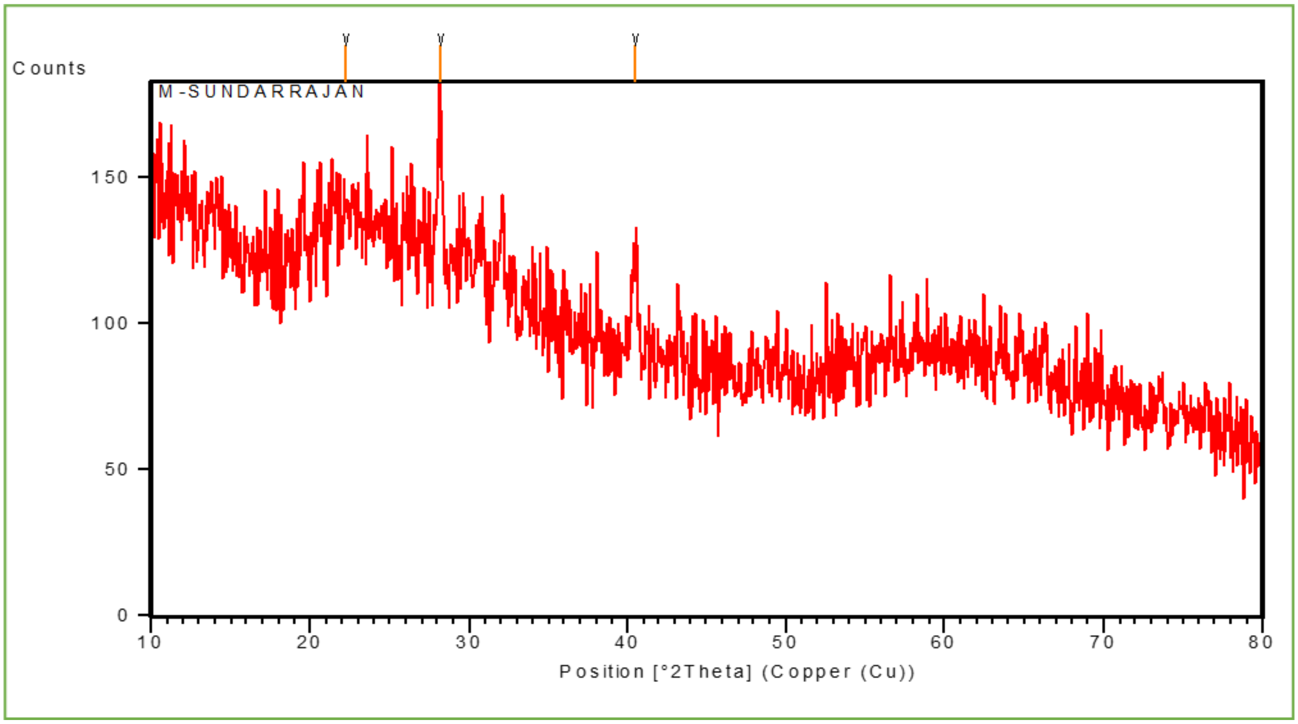

Fig.3.3 XRD Spectrum of CDC nanofluid

defects and functional groups, a typical feature imparting high surface activity and tunable optoelectronic properties to the nanoparticles(49).

The second significant peak at 28.19° 2θ, corresponding to a d-spacing of 3.165 Å, is indicative of enhanced crystalline order or possibly the co-existence of doped phases. This may arise from nitrogen or oxygen heteroatom dopants within the graphitic matrix or the presence of minor metal oxide impurities, as observed in related materials. The sharper intensity suggests increasing crystallinity relative to the amorphous baseline, which could facilitate charge transport and improved material stability. (47, 50)

Additionally, the reflection at 40.42° 2θ corresponding to a 2.231 Å d-spacing typically belongs to crystalline metal oxide phases integrated into the carbon matrix to form nanohybrids. This is corroborated by literature reports on carbon-metal oxide composite nanoparticles, where such peaks reflect well-defined crystal facets contributing to catalytic or sensing enhancement.(46)

In total, the XRD data supports a composite nanostructure dominated by amorphous carbon dots with sporadic crystalline graphitic regions and embedded metal oxide nanoparticles or doped carbon phases. This hybrid arrangement aligns with contemporary green synthesis routes for

multifunctional carbon nanomaterials, linking structural characteristics with the desired physicochemical properties for applications in catalysis, sensing, and optoelectronics.

3.4. Particle Size analysis

Results and discussion

Dynamic light scattering analysis reveals that the hydrodynamic diameter of the synthesized carbondot clusters is 235.9 nm, with a polydispersity index (PDI) of 34.8% and a diffusion coefficient of 2.1 $\mu m^2/s$. The sample shows a transmittance of 71.3%.

The intensity-based particle size distribution demonstrates three distinct peaks: a major fraction at 85.78 nm (area 51.72%), a secondary population at 398.6 nm (area 44.23%), and a small proportion of larger aggregates at 4441 nm (area 4.05%) with corresponding standard deviations of 18.57 nm, 102.53 nm, and 450.3 nm, respectively. These values reflect a wide size distribution in the aqueous dispersion.

The major particle size fraction around 85.78 nm revealed by the intensity-based particle size distribution of the synthesized carbon dot clusters supports the presence of nanostructures suitable for

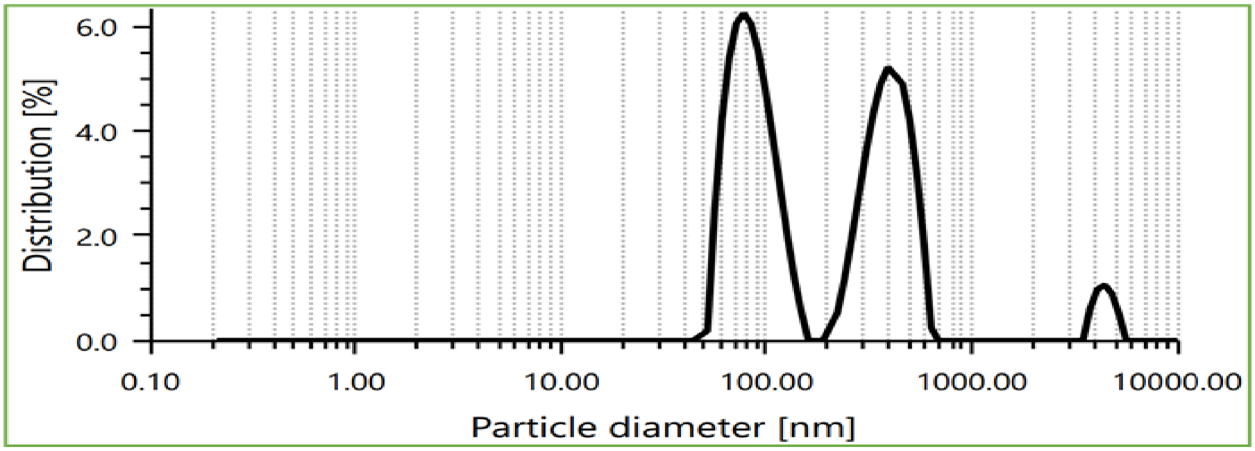

Fig.3.4. Particle size analysis of CDC nanofluid by DLS method

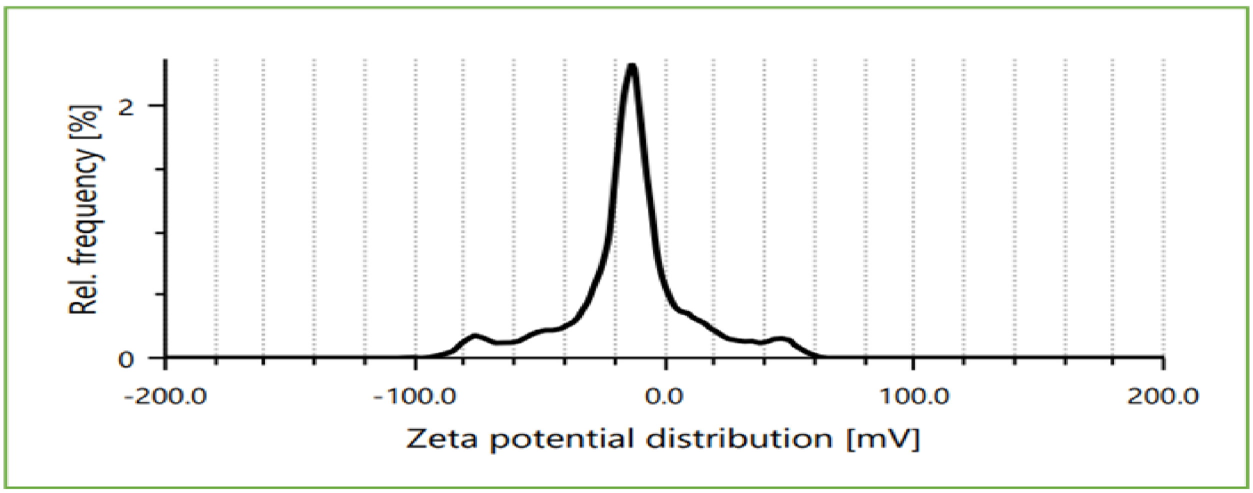

Fig.3.5. Zeta potential analysis of CDC nanofluid

nanotechnology applications. While this size is slightly larger than some reported ultra-small carbon dots (~1–12 nm), carbon dots in the 5–100 nm range have also been frequently documented and demonstrated functional properties such as fluorescence and catalytic activity (50).

The predominance of this major peak suggests that the sample exhibits a substantial population of nanoparticles within the nanoscale regime, contributing beneficially to the surface-to-volume ratio and quantum confinement effects important for optoelectronic and biomedical uses. Clusters or larger size distributions, such as peaks observed at 398.6 nm and 4441 nm, likely result from particle agglomeration or secondary aggregation phenomena.

Such behaviors are common in nanomaterial suspensions, especially when surface stabilization and passivation are limited and have been similarly reported in biomass-derived nanocarbon syntheses with varied particle sizes and distribution widths (51, 50).

The measured hydrodynamic diameter (235.9 nm) and size distribution peaks highlight a broader and larger sizing profile compared to most green-synthesized carbon dots, which generally fall in the range of 1–12 nm and present much narrower PDIs. This contrast may suggest that the sample investigated here contains carbon dot aggregates or larger clusters possibly resulting from agglomeration or incomplete passivation during synthesis(51 50).

The polydispersity index in this work, at 34.8%, points towards moderate to high particle size heterogeneity, which is less optimal for fluorescence, sensing, or bioimaging applications where mono dispersity is advantageous.

Literature also documents larger aggregates in carbon-based nano-dispersions, particularly when hydrodynamic size is measured rather than dry particle size where agglomerates can raise mean diameters well above the quantum dot regime (48, 49, 52, 53). These works reinforce the interpretation that while most carbon dot syntheses yield primary particles in the range of 1–12 nm, hydrodynamic diameters can increase dramatically depending on sample concentration, aging, or insufficient surface passivation (51, 50).

Overall, focusing on the nano-sized fraction around 85 nm, it is consistent with functional carbon dot clusters reported across the literature, affirming that the synthesized material maintains nanoscale features while recognizing that secondary larger aggregates may influence the dispersion properties and application performance if not controlled.

3.5 Zeta Potential

Results and discussion

The zeta potential measurement for the synthesized carbon dot clusters reveals a mean value of –18.1 mV, with a distribution peak at –12.6 mV and a standard deviation of 1.6 mV. Electrophoretic mobility is recorded as –14120 $\mu m^2 cm/Vs$, and the measured conductivity is 0.907 mS/cm. These values reflect the overall surface charge and dispersion stability of the nanomaterial in aqueous medium.

Discussion

The observed mean zeta potential of –18.1 mV signifies that the carbon dot clusters are moderately stable in aqueous dispersions, as values greater than ±30 mV typically correspond to highly stable colloidal systems due to strong electrostatic repulsion. While this value is slightly less negative than the –20 to –30 mV range frequently obtained for optimally dispersed green-synthesized carbon dots, it is well identified that they are moderately stable.

The zeta potential of the synthesized carbon dot clusters, while not maximally negative, is well suited for dispersions that are stable enough for catalysis, photonics, or environmental remediation provided that the formulation and concentration are optimized for minimal aggregation. A distribution peak at –12.6 mV may indicate a secondary, slightly less stable subpopulation or the presence of larger, less surface-functionalized aggregates, which is not uncommon in multi-modal particle distributions resulting from green or bio-waste-based synthesis methods (54, 55).

In summary, the moderate negative zeta potential underscores adequate colloidal stability in the current sample, comparable to several previously published carbon dot systems prepared from biological or green precursors. Further surface modification or post-synthesis treatments could push the stability higher if required for advanced biological or technological applications.

3.6 Scanning Electron Microscopy

Results and discussion

Scanning Electron Microscopy (SEM) analysis clearly reveals the formation of nanoscale clusters within the carbon dot nanofluid sample. The recorded SEM micrograph shows a distribution of nearly spherical aggregates. Several representative clusters were measured, with particle diameters ranging from approximately 67.6 nm to 88.9 nm. For instance, particle 1 (Pa1) exhibits a diameter of 75.1 nm, while particle 3 (Pa3) is larger at 88.9 nm. The measured particle diameter and orientation angles indicate some variability in cluster size and orientation within the sample. These nanoclusters appear uniformly distributed, with limited aggregation, a characteristic favorable for nanofluid stability.

The SEM results confirm the successful synthesis and dispersion of carbon dot clusters at the nanoscale. The particle size distribution, with most aggregates between 67–89 nm, aligns well with expectations for carbon dot-based nanofluids (54). Uniformity and limited agglomeration suggest effective stabilization, which may be attributed to the synthesis protocol, precursor choice, or surface capping agents employed. The observed morphology, with spherical particle shapes and moderate orientation angles, indicates homogeneous nucleation and growth during synthesis (52,54). These physical characteristics support enhanced colloidal stability and are likely to improve the thermal and optical properties of the nanofluid. Comparing these results with similar carbon dot clusters from previous studies, the measured sizes fall within reported ranges, but the noted cluster uniformity and dispersion may offer improved performance for applications in heat transfer, sensing, or bio-imaging.

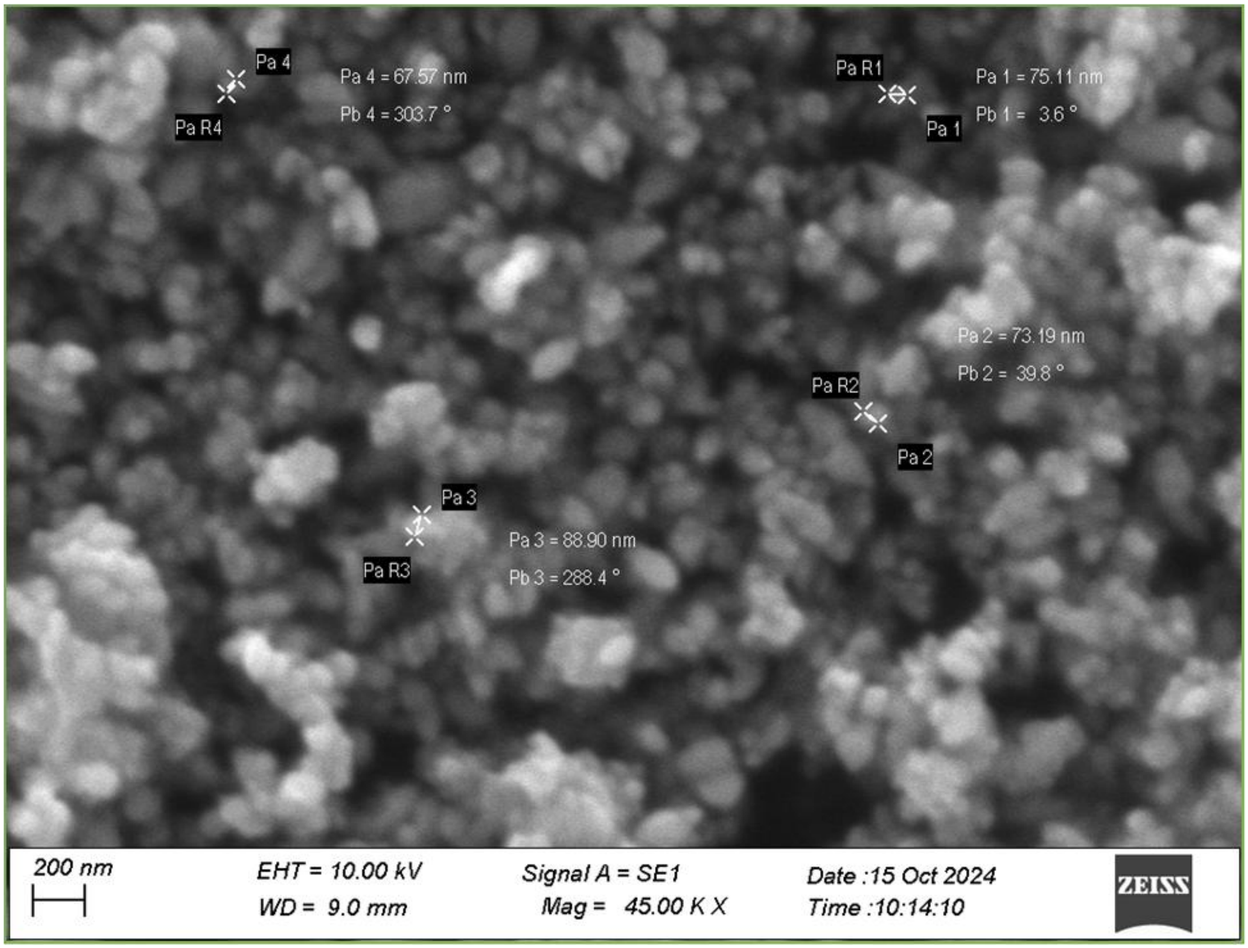

Fig.3.6. SEM analysis of CDC nanofluid

REFERENCES

[1] Stewart, S.; Wei, Q.; Sun, Y. Surface chemistry of quantum-sized metal nanoparticles under light illumination. Chemical Science, 2021, 12, 1227-1239. https://doi.org/10.1039/D0SC04651E

[2] Joudeh, N., Linke, D. Nanoparticle classification, physicochemical properties, characterization, and applications: a comprehensive review for biologists. J Nanobiotechnol 20, 262 (2022). https://doi.org/10.1186/s12951-022-01477-8

[3] K. S. Novoselov, V. I. Fal′ko, L. Colombo, P. R. Gellert, M. G. Schwab and K. Kim, A roadmap for graphene, Nature, Vol. 490, 192–200, (2012).

[4] Ce Zhao, Liuyang Xiao, Zhexue Chen and Yong Zhang, Extremely Downsized Materials: Ball-Milling-Enabled Universal Production and Size-Reduction-Induced Performance Enhancement, Acc. Mater. Res. 2024, 5, 12, 1583–1597, https://doi.org/10.1021/accountsmr.4c00306

[5] Jiang Z, Li L, Huang H, He W, Ming W. Progress in Laser Ablation and Biological Synthesis rocesses: “Top-Down” and “Bottom-Up” Approaches for the Green Synthesis of Au/Ag Nanoparticles.Int.J.Mol.Sci..,2022;23(23):14658. https://doi.org/10.3390/ijms232314658.

[6] Sonawane, L.D., Mandawade, A.S., Gite, A.B. et al. Sol–gel synthesis of silicon oxide (SiO2) nanoparticles: exploring gas sensing and photocatalytic applications. J Mater. Sci: Mater Eng. 20, 8 (2025). https://doi.org/10.1186/s40712-025-00209-8

[7] Li Luo, Wan Huang, Jun Zhang, Yao Yu and Taolei Sun, Metal-Based Nanoparticles as Antimicrobial Agents: A Review,ACS Appl. Nano Mater. 2024, 7, 3, 2529–2545 https://doi.org/10.1021/acsanm.3c05615.

[8] Naseem, Khalida, Aziz, Asad, Khan, Mohammad Ehtisham, Ali, Shahzaib and Khalid, Awais. "Bioinorganic metal nanoparticles and their potential applications as antimicrobial, antioxidant and catalytic agents: a review" Reviews in Inorganic Chemistry, vol. 45, no. 1, 2025, pp. 207-236. https://doi.org/10.1515/revic-2023-0040

[9] Maximilian A. Beach, Umeka Nayanathara, YantingGao, Changhe Zhang, YijunXiong, Yufu Wang and Georgina K. Such, Polymeric Nanoparticles for Drug Delivery, Chem. Rev. 2024, 124, 9, 5505–5616, https://doi.org/10.1021/acs.chemrev.3c00705

[10] Musa, A. A., Bello, A., Adams, S. M., Onwualu, A. P., Anye, V. C., Bello, K. A., &Obianyo, I. I. (2025). Nano-Enhanced Polymer Composite Materials: A Review of Current Advancements and Challenges, Polymers, 17(7), 893. https://doi.org/10.3390/polym17070893

[11] Khan, I., Saeed, K., & Khan, I. (2019). Nanoparticles: Properties, applications and toxicities. Arabian Journal of Chemistry, 12(7), 908–931.https://doi.org /10.1016/ j.arabjc. 2017. 05.011

[12] P.AbdulRasheed, MenonAnkitha, Vijayamohanan K. Pillai and Subbiah Alwarappan, Graphene quantum dots for biosensing and bioimaging, RSC Adv.,2024,14,16001-16023, https://doi.org/ 10.1039/ D4RA01431F.

[13] ZawarAlam Qureshi, Hanan Dabash, Deepalekshmi Ponnamma, M.K.G. Abbas, Carbon dots as versatile nanomaterials in sensing and imaging: Efficiency and beyond, Heliyon, Volume 10, Issue 11, 2024, e31634, https://doi.org/10.1016/j.heliyon.2024.e31634.

[14] Moustafa A. Darwish, WalaaAbd-Elaziem, Ammar Elsheikh, Abdelhameed A. Zayed, Advancements in nanomaterials for nanosensors: a comprehensive review, Nanoscale Advances, Volume 6, Issue 16, 2024, Pages 4015-4046, https://doi.org/10.1039/d4na00214h.

[15] Sánchez-López, Elena, Daniela Gomes, Gerard Esteruelas, Lorena Bonilla, Ana Laura Lopez-Machado, Ruth Galindo, Amanda Cano, Marta Espina, Miren Ettcheto, Antoni Camins, and et al. 2020. "Metal-Based Nanoparticles as Antimicrobial Agents: An Overview" Nanomaterials 10, no. 2: 292. https://doi.org/10.3390/nano10020292.

[16] Sun, L., Geng, J., Dong, K., & Sun, Q. (2024). An Experimental Study on the Effect of Nanofluids on the Thermal Conductivity and Rheological Properties of a Coolant for Liquids. Energies,17(6),1313. https://doi.org/10.3390/ en17061313

[17] Kiran Bijapur, Samir Mandal, P. G. Siddheshwar, Suryasarathi Bose and Gurumurthy Hegde, Experimental investigation of a biomass-derived nanofluid with enhanced thermal conductivity as a green, sustainable heat-transfer medium and qualitative comparison via mathematical modelling, Nanoscale Adv., 2024, 6, 4944-4955, DOI: 10.1039/D4NA00362D

[18] Wei Yu and HuaqingXie, A Review on Nanofluids: Preparation, Stability Mechanisms, and Applications, Journal of Nanomaterials, Volume 2012, (2011), Article ID 435873, doi:10.1155/2012/435873

[19] Duygu Yılmaz Aydın and Metin Gürü, Nanofluids: preparation, stability, properties, and thermal performance in terms of thermo-hydraulic, thermodynamics and thermo-economic analysis, Journal of Thermal Analysis and Calorimetry, Volume 147, pages 7631–7664,(2022), https://doi.org/10.1007/ s10973-021-11092-8

[20] Muhammad Usman Sajid, Yusuf Bicer, Impacts of ultrasonication time and surfactants on stability and optical properties of CuO, Fe3O4, and CNTs/water nanofluids for spectrum selective applications, Ultrasonics Sonochemistry, Volume 88, 2022, 106079, https://doi.org/10.1016/j.ultsonch.2022.106079.

[21] Fatemeh Seifikar, Saeid Azizian, Super-stable carbon quantum dots nanofluid for efficient solar-thermal conversion, Energy Conversion and Management, Volume 228, 2021, 113675, https://doi.org/10.1016/j.enconman.2020.113675

[22] Trong Tam, N., Viet Phuong, N., Hong Khoi, P., Ngoc Minh, P., Afrand, M., Van Trinh, P., Hung

Thang, B., Żyła, G., & Estellé, P. (2020). Carbon Nanomaterial-Based Nanofluids for Direct Thermal Solar Absorption. Nanomaterials, 10(6), 1199. https://doi.org/10.3390/nano10061199

[23] Mahani M, Montazer L, Khakbaz F, Divsar F, Yoosefian M. Photothermal performance of a novel carbon dot and its conjugate with disulfiram for prostate cancer PC3 cell therapy. Nanomedicine, 2023, 18(24):1703-1718. doi: 10.2217/nnm-2023-0195

[24] Dean Chou, Ali Rehman, Mustafa Inc&ShahramRezapour, Examination of heat transfer in carbon nanotube nanofluids under thermal radiation, magnetic field, and viscosity distribution. Multiscale and Multidiscip. Model. Exp. and Des. 8, 237 (2025). https://doi.org /10.1007/s41939-025-00819-x

[25] Hamid-Reza Bahrami, OmidAllahdadi, Hamid Saffari, Nanofluids for advanced thermal management: A multi-criteria review of performance, cost, and environmental impacts, Results in Materials, Volume 27, 2025, 100753, https://doi.org/10.1016/j.rinma.2025.100753.

[26] Shakeel Ahmed, Saifullah, Mudasir Ahmad, BabuLal Swami, SaiqaIkram, Green synthesis of silver nanoparticles using Azadirachta indica aqueous leaf extract, Journal of Radiation Research and Applied Sciences, Volume 9, Issue 1,2016, Pages1-7, https://doi.org/10.1016/j.jrras.2015.06.006.

[27] Aditya Amrut Pawar, Jyotirmayee Sahoo, AakashVerma, Abdullah M. Alswieleh, Abhijit Lodh, Rajesh Raut, Jaya Lakkakula, Byong-Hun Jeon, Md. Rabiul Islam, Azadirachta indica-Derived Silver Nanoparticle Synthesis and Its Antimicrobial Applications, Journal of Nanomaterials,(2022), https://doi.org/10.1155/ 2022/ 4251229

[28] Harmeet Kaur Kohli, DeepaParab, Green synthesis of carbon quantum dots and applications: An insight, Next Materials, Volume 8,2025,100527, https://doi.org/10.1016/ j.nxmate.2025.100527.

[29] Kannan Vellaisamy, Ayerathal Velmurugan, Esakkimuthu Shanmugasundaram, Nithesh Kumar Krishnan, Vaseeharan Baskaralingam, Ashokkumar Sibiya and Stalin Thambusamy, Synthesis of carbon quantum dots from neem fruit flesh for dual metal sensing, bioimaging, and antibacterial applications, New J. Chem., 2025,49,8413-8427, https://doi.org/ 10.1039 /D5NJ00292C.

[30] Asma Ben Amor, Hadia Hemmami, Mohammed Taher Gherbi, Bachir Ben Seghir, Soumeia Zeghoud, Ahlam Hacine Gharbi, Djihad Chenna, Ilham Ben Amor, Huda Alsaeedi, David Cornu, Mikhael Bechelany& Ahmed Barhoum, Synthesis of spherical carbon nanoparticles from orange peel and their surface modification with chitosan: Evaluation of optical properties, biocompatibility, antioxidant and anti-hemolytic activity. Biomass Conv. Bioref. 15, 11345–11358 (2025). https://doi.org/10.1007/s13399-024-06291-w

[31] Tavishi Chopra and Raman Parkesh, Microwave-Assisted Synthesis of Functionalized Carbon Nanospheres Using Banana Peels: pH-Dependent Synthesis, Characterization, and Selective Sensing Applications, ACS Omega 2024, 9, 4, 4555–4571, https://doi.org/ 10.1021 / acsomega.3c07544

[32] Merat Karimi, Mina Homayoonfal, Mostafa Zahedifar, Amirreza Ostadian, Reyhaneh Adibi, Bahareh Mohammad zadeh, Arash Raisi, Fatemeh Ravaei, Somaye Rashki, Mahsa Khakbraghi, Michael Hamblin, Zahra Kheirkhah, EhsanSadeghi, Majid Nejati & Hamed Mirzaei, Development of a novel nanoformulation based on aloe vera-derived carbon quantum dot and chromium-doped alumina nanoparticle (Al2O3:Cr@Cdot NPs): evaluating the anticancer and antimicrobial activities of nanoparticles in photodynamic therapy. Cancer Nano15, 26, (2024). https://doi.org /10.1186/ s12645-024-00260-8

[33] Kiran Bijapur, Samir Mandal, P. G. Siddheshward, Suryasarathi Bose and GurumurthyHegde, Unlocking efficiency: experimental and theoretical insights into biomass-derived carbon nanofluids with enhanced thermal conductivity, Nanoscale, 2025, 17, 10239-10249, DOI: 10.1039/D4NR04740K.

[34] Zahra Nezafat, Yahao Dong, Mahmoud Nasrollah zadeh, NasrinShafiei, Hanieh Gharoubi and ShahrzadJavanshir, Recent progress in energy conversion and storage of agricultural waste-derived (carbon/nano)

materials: a review, Green Chem., 2024, 26, 10687-10717, DOI: 10.1039 /D3GC04332K.

[35] Yasser Elhenawy, Kareem Fouad, Ahmed Refaat, Osama A. Al-Qabandi, Monica Toderaș, Mohamed Bassyouni, Experimental Enhancement of Thermal and Electrical Efficiency in Concentrator Photovoltaic Modules Using Nanofluid Cooling, Energy Science & Engineering, Volume13, Issue4, 2025, Pages 1492-1508, https://doi.org/10.1002/ese3.2026

[36] Zainon, S. N. M., & Azmi, W. H. (2021). Recent Progress on Stability and Thermo-Physical Properties of Mono and Hybrid towards Green Nanofluids. Micromachines, 12(2), 176. https://doi.org/10.3390/mi12020176

[37] Ali, N., Bahman, A. M., Aljuwayhel, N. F., Ebrahim, S. A., Mukherjee, S., &Alsayegh, A. (2021). Carbon-Based Nanofluids and Their Advances towards Heat Transfer Applications—A Review. Nanomaterials, 11(6), 1628. https://doi.org/10.3390/nano11061628

[38] M. Moghaddari, F. Yousefi, S. Aparicio, S.M. Hosseini, Thermal conductivity and structuring of multiwalled carbon nanotubes based nanofluids, Journal of Molecular Liquids, Volume 307, 2020, 112977, https://doi.org/10.1016/j.molliq.2020.112977.

[39] Nizam, N.U.M., Hanafiah, M.M., Mahmoudi, E. et al. Synthesis of highly fluorescent carbon quantum dots from rubber seed shells for the adsorption and photocatalytic degradation of dyes. Sci Rep 13, 12777 (2023). https://doi.org/10.1038/s41598-023-40069-w

[40] Costa, A. I., Barata, P. D., Moraes, B., &Prata, J. V. (2022). Carbon Dots from Coffee Grounds: Synthesis, Characterization, and Detection of Noxious Nitroanilines. Chemosensors,10(3) ,113. https: // doi.org / 10.3390 / chemosensors10030113.

[41] Sailaja Prasannakumaran Nair, Smrithi; Kottam, Nagaraju; S G, Prasanna Kumar. (2020). Green Synthesized Luminescent Carbon Nanodots for the Sensing Application of Fe3+ Ions. Journal of Fluorescence, doi:10.1007/s10895-020-02505-2

[42] Setianto S, Men LK, Bahtiar A, Panatarani C, Joni IM. Carbon quantum dots with honeycomb structure: a novel synthesis approach utilizing cigarette smoke precursors. Sci Rep. 2024 Jan 23;14(1):1996. doi: 10.1038/s41598-024-52106-3.

[43] Ma, X., Li, S., Hessel, V., Lin, L., Meskers, S., &Gallucci, F. (2019). Synthesis of luminescent carbon quantum dots by microplasma process. Chemical Engineering and Processing: Process Intensification, 140, 29-35.

[44] Magagula, L. P., Masemola, C. M., Motaung, T. E., Moloto, N., & Linganiso-Dziike, E. C. (2025). Synthesis of Cellulose-Based Fluorescent Carbon Dots for the Detection of Fe(III) in Aqueous Solutions. Processes, 13(1), 257. https://doi.org/ 10.3390/pr13010257

[45] Fawaz, W., Hasian, J. & Alghoraibi, I. Synthesis and physicochemical characterization of carbon quantum dots produced from folic acid. Sci Rep 13,18641(2023). https://doi.org/ 10.1038/ s41598-023- 46084-1

[46] De Lima, S.R.; Costa, T.V.; Santos, T.T.S.; Felipe, D.G.; Serna, T.B.; Andrade, A.A.; Pilla, V. Optical Characterization of Fluorescent Chitosan-Based Carbon Dots Embedded in Aqueous Natural Dye. Colorants 2024, 3, 269–281. https:// doi.org/10.3390/colorants3040019

[47] Mahdavi, B., Koushki, E., NooriDolouie, B., &Mohammad hosseini, M. (2024). Green synthesis of carbon quantum dots and its composite with Ag/chitosan using citrus fruit extracts. Trends in Phytochemical Research, 8(2), 141-148. https://doi.org/10.71596/ tpr.2024. 112608

[48] Qureshi, Z. A., Dabash, H., Ponnamma, D., & Abbas, M. K. G. (2024). Carbon dots as versatile nanomaterials in sensing and imaging: Efficiency and beyond. Heliyon, 10(11), https://doi.org/10.1016/j.heliyon.2024.e31634

[49] Huo, X., He, Y., Ma, S., Jia, Y., Yu, J., Li, Y., & Cheng, Q. (2020). Green Synthesis of Carbon Dots from Grapefruit and Its Fluorescence Enhancement. Journal of Nanomaterials, 2020, Article ID 8601307, 10 pages. https://doi.org/10.1155/2020/8601307

[50] Jlassi, K., Eid, K., Sliem, M.H. et al. Rational synthesis, characterization, and application of environmentally friendly (polymer–carbon dot) hybrid composite film for fast and efficient UV-assisted Cd^{2+} removal from water. Environ SciEur 32, 12 (2020). https://doi.org/10.1186/ s12302-020-0292-z

[51] Gao, Y., & Cheng, F. (2025). One-Step Green Synthesis of Functionalized Carbon Dots from Five Edible Mushrooms. Spectroscopy Online, May, 2025

[52] Sivamaran V, Balasubramanian V, Gopalakrishnan M, Viswabaskaran V, Rao AG. Combined synthesis of carbon nanospheres and carbon nanotubes using thermal chemical vapor deposition process. ChemPhys Impact. 2022; 4:100072. doi: 10.1016/j.chphi.2022.100072

[53] Bhandari, S., Roy, A., Ali, M.S. et al. Cotton soot derived carbon nanoparticles for NiO supported processing temperature tuned ambient perovskite solar cells. Sci Rep 11, 23388 (2021). https://doi.org/10.1038/s41598-021-02796-w

[54] Jing, H. H., Bardakci, F., Akgöl, S., Kusat, K., Adnan, M., Alam, M. J., Gupta, R., Sahreen, S., Chen, Y., Gopinath, S. C. B., &Sasidharan, S. (2023). Green Carbon Dots: Synthesis, Characterization, Properties and Biomedical Applications. Journal of Functional Biomaterials, 14(1), 27. https://doi.org/10.3390/jfb14010027

[55] Hoan, BuiThi, Tam, Phuong Dinh, Pham, Vuong-Hung, Green Synthesis of Highly Luminescent Carbon Quantum Dots from Lemon Juice, Journal of Nanotechnology, 2019, 2852816, 9 pages, 2019. https://doi.org/ 10.1155/2019 /2852816.